Pergamon

Geochimica et Cosmochimica Acta, Vol. 59, No. 19, pp. 3917–3927, 1995

0016-7037/95 $9.50 + .00

0016-7037(95)00265-0

Chemistry and origin of mantle sulfides in spinel peridotite xenoliths from alkaline basaltic lavas, Nógrád-Gömör Volcanic Field, northern Hungary and southern Slovakia*

Cs. Szabó[1,2] and R. J. Bodnar[1]

[1]Fluids Research Laboratory, Department of Geological Sciences, Virginia Polytechnic Institute and State University, Blacksburg, VA 24061, USA

[2]Department of Petrology and Geochemistry, Eötvös University, Budapest, Múzeum Krt. 4/A, 1088, Hungary

(*Received October* 6, 1994; *accepted in revised form June* 4, 1995)

Abstract—Neogene to Quaternary alkaline basalts from the Nógrád-Gömör Volcanic Field (NGVF) in the Carpathian-Pannonian Region of northern Hungary and southern Slovakia contain a large number and great variety of sulfide-bearing mantle xenoliths. A previous detailed textural and chemical study of spinel peridotite (Cr-diopside) xenoliths from the NGVF identified multiple mantle processes (i.e., partial melting(s), metasomatism, and entrainment of the peridotite xenoliths into the host lavas), which might be genetically associated with sulfides and which could account for their variability in texture and chemistry.

Eleven spinel peridotite nodules (three protogranular to porphyroclastic, three equigranular, four secondary recrystallized, and one strongly metasomatized xenolith) were selected to characterize the sulfide assemblages. Two types of primary sulfide grains and two types of secondary sulfide grains were identified based on occurrence and distribution. Type-i primary sulfide assemblages are interstitial to mantle silicates, whereas Type-e primary sulfide assemblages are enclosed in mantle silicates. Secondary sulfides are connected either to healed fractures in mantle silicates (Type-f) or to borders of mantle silicates (Type-b).

Type-i and Type-e primary sulfide assemblages consist mostly of the phases pentlandite (Pn), chalcopyrite (Cp), monosulfide solid solution (MSS), and violarite (Vi). Type-f and Type-b secondary sulfide grains are indistinguishable mineralogically and chemically from the Type-i and Type-e sulfide assemblages, but can be distinguished based on texture and occurrence.

MSS sulfide blebs in the metasomatized xenolith developed their compositions and textures as a result of mantle metasomatism. Sulfides in the protogranular/porphyroclastic, equigranular, and recrystallized xenoliths represent immiscible melts trapped during partial melting event(s) in the mantle. In the less deformed (protogranular/porphyroclastic) xenoliths the Cp + Pn assemblage (either Type-e or Type-i) crystallized from a Cu-Ni-bearing sulfide liquid which was in equilibrium with MSS at high temperature. In addition, an MSS + Cp + Pn assemblage (either Type-e or Type-i) was produced as a result of exsolution of Cp and Pn from the high-temperature MSS during cooling. In the more deformed equigranular and recrystallized xenoliths Pn + MSS or Pn ± Cp ± Po are present.

The abundance of sulfide assemblages in individual samples can be correlated to the texture of the xenoliths. The protogranular/porphyroclastic and metasomatized xenoliths show sulfide concentrations up to 0.5 vol%, whereas the other xenoliths have less than 0.02 vol% sulfides. This correlation between sulfide abundance and textural type of host xenolith indicates that the heterogeneous distribution of sulfides within the upper mantle is related, at least in part, to deformation and recrystallization processes.

1. INTRODUCTION

The study of alkaline basalt- and kimberlite-hosted spinel peridotite xenoliths yields insights into processes occurring in the upper mantle. Many such nodules from around the world have been extensively studied petrographically, mineralogically, chemically, and isotopically during the past few decades. However, many aspects of these nodules, including the nature and origin of contained sulfide assemblages, are poorly understood. It is generally accepted that these sulfides can provide information relevant to understanding processes such as mantle depletion and enrichment, as well as the origin of Fe-Ni-Cu sulfide ore bodies. Nevertheless, relatively few papers have been published describing sulfide assemblages from alkaline basalt-hosted xenoliths (e.g., De Waal and Calk, 1975; Lorand and Conquéré, 1983; Dromgoole and Pasteris, 1987) and from kimberlite-hosted xenoliths (e.g., Frick, 1973; Desborough and Czamanske, 1973; Bishop et al., 1975; Meyer and Boctor, 1975).

The goal of the present paper is to provide petrographic, mineralogical, and chemical constraints on the origin of sulfide assemblages from a petrologically and geochemically well-characterized suite of spinel peridotite (Cr-diopside) xenoliths from the Nógrád-Gömör Volcanic Field (NGVF) of northern Hungary and southern Slovakia. These data preserved in peridotite xenoliths provide a better understanding of upper mantle processes and record the history of the evolution of the mantle beneath the Nógrád-Gömör Volcanic Field.

2. GEOLOGIC BACKGROUND AND SAMPLE DESCRIPTION

The Nógrád-Gömör Volcanic Field is located within the Carpathian-Pannonian Region of Eastern Europe (Fig. 1). The field is com-

* Presented at the fifth biennial Pan-American Conference on Research on Fluid Inclusions (PACROFI V) held May 19–21, 1994, at the Instituto de Investigaciones Electricas in Cuernavaca, Morelos, Mexico.

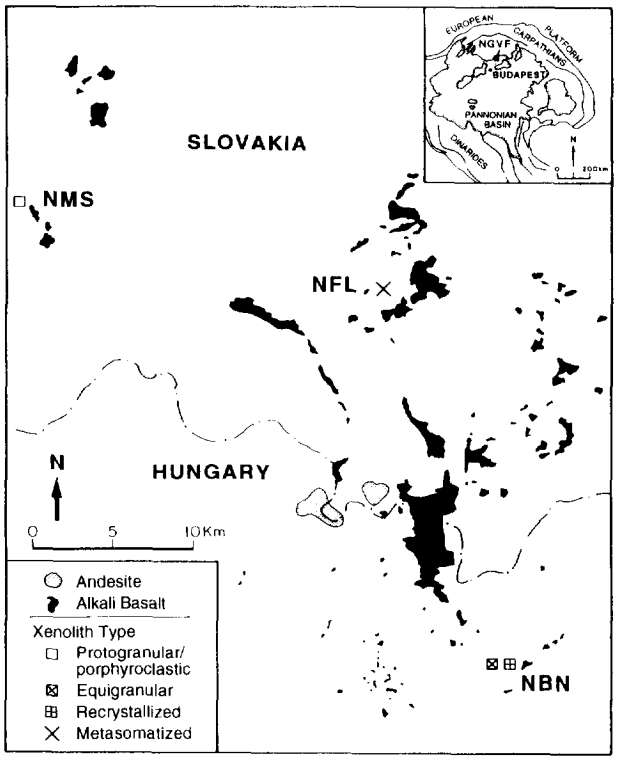

FIG. 1. Simplified map of the Nógrád-Gömör Volcanic Field (NGVF, inset) showing the locations of the Cr-diopside xenoliths studied. NMS = Maskófalva-Maskova; NFL = Fülek-Fil'akovo – Kercsiktetö; NBN = Bárna – Nagykö. The textural type(s) of xenoliths studied from each location are also shown.

posed of Neogene to Quaternary alkaline basalts which contain a large number and great variety of mantle nodules with different sulfide assemblages. Minor xenolith-free Miocene andesites are also present.

Based on a detailed textural and chemical study of Cr-diopside peridotite xenoliths from the Nógrád-Gömör Volcanic Field (Szabó and Taylor, 1991, 1994), the nodules provide evidence for at least three common upper mantle processes which occurred beneath the NGVF. Each of these processes may be genetically associated with sulfides in the nodules and may account for their variability in texture and chemistry. These three processes are: (1) partial melting, (2) mantle metasomatism (evidenced by mantle veinlets and by metasomatic amphiboles and phlogopites), and (3) entrainment of the peridotite xenoliths into the host alkali basalts.

For this study eleven Cr-diopside peridotite nodules were selected from a previously well-studied upper mantle xenolith suite. This suite represents the heterogeneous subcontinental upper mantle beneath the Nógrád-Gömör Volcanic Field (Szabó and Taylor, 1994). These samples also contain all of the various types of sulfide assemblages identified from the upper mantle beneath the NGVF (Fig. 1). The eleven xenoliths include:

1) Three protogranular to porphyroclastic, relatively undepleted, and slightly deformed xenoliths composed of amphibole-bearing spinel lherzolite to spinel websterite from Maskófalva-Maskova (location NMS on Fig. 1). These are hereafter referred to as protogranular/porphyroclastic xenoliths.
2) Three equigranular, depleted, and strongly deformed xenoliths composed of anhydrous spinel lherzolite from Bárna-Nagykö (location NBN on Fig. 1). These are hereafter referred to as equigranular xenoliths.
3) Four secondary recrystallized, strongly depleted xenoliths composed of anhydrous spinel lherzolite to phlogopite-bearing dunite also from locality NBN. These are hereafter referred to as recrystallized xenoliths.
4) One equigranular, strongly metasomatized xenolith composed of amphibole peridotite from Fülek-Fil'akovo-Kercsiktetö (locality NFL on Fig. 1). This is hereafter referred to as the metasomatized xenolith.

The abundance of sulfide assemblages in individual samples varies according to the textural types of upper mantle peridotite xenoliths. The protogranular/porphyroclastic and metasomatized xenoliths show a very high abundance of sulfide (~0.5 vol%), whereas the equigranular and recrystallized xenoliths have lower abundances (<0.02 vol%) of sulfide.

3. ANALYTICAL TECHNIQUES

Sulfide assemblages were examined in reflected light using high-magnification oil-immersion objectives to identify different phases of the sulfide assemblages and to estimate their modal proportions. Analyses of the sulfides were performed using a CamScan SEM system equipped with an HNU energy-dispersive Si(Li) detector. Operating conditions were 20 kV accelerating potential, 0.5-nanoamp sample current, 100-second counting (live) times for S, Fe, Ni, Co, and Cu analyzed in each sulfide assemblage. Raw data were corrected using the Zap II analytical program provided by the vendor. Details of this method are presented in Gedcke et al. (1982).

Bulk sulfide compositions of samples were estimated by combination of modal proportions of the sulfide phases and average chemical compositions of the individual phases making up the Type-i and Type-e (defined below) sulfide assemblages. Modal proportions were visually estimated using reflected light microscopy. The error associated with such determinations has been estimated to be approximately 10% using the method of De Waal and Calk (1975). A broad electron beam was also used in an attempt to obtain bulk chemical analyses of the sulfide assemblages, but it proved to be inadequate because chalcopyrite often occurs at the edge of the sulfide assemblages (Fig. 2C to E) and, therefore, outside of the area of the beam. Note that when violarite was present, we added its modal proportion to that of pentlandite to calculate the bulk sulfide composition due to uncertainties in the origin and chemistry of the violarite as discussed below.

4. SULFIDE ASSEMBLAGE PETROGRAPHY

The following four distinct types of sulfide assemblages have been identified based on texture, size, and location within the xenolith:

1) Type-e: Isolated single inclusions of sulfide with spherical (or rarely elongated) habits enclosed in olivine, orthopyroxene and, rarely, in spinel (Fig. 2A, 2D, and 2F) and amphibole (Fig. 2G). Grain-size varies from 10–100 μm. Four to five inclusions are commonly found in each thin section of the protogranular/porphyroclastic and the metasomatized xenoliths, whereas one or two sulfide blebs per thin section is a common average value for the equigranular and recrystallized xenoliths.
2) Type-i: Interstitial, anhedral sulfide grains with curvilinear (Fig. 2B and 2E) or linear (Fig. 2C) boundaries; they range from 50–220 μm in diameter. These sulfide assemblages appear mostly in the protogranular/porphyroclastic xenoliths where six to seven grains per thin section is an average value. In contrast, only one or two sulfide inclusions are observed in thin sections of the equigranular and recrystallized xenoliths.
3) Type-f: Small (1–15 μm in diameter) spherical blebs or negative crystal-shaped inclusions along inter- or intragranular healed fractures (Fig. 2H). These sulfides are

sometimes associated with CO_2 and multiphase melt inclusion arrays. These trails frequently crosscut olivines and orthopyroxenes and are most common in the protogranular/porphyroclastic xenoliths. Sometimes the cracks intersect Type-e sulfide inclusions to form Type-f sulfide inclusions (Fig. 2G).

4) Type-b: Spherical or irregular, small (1–15 μm in diameter) sulfide blebs at borders of major mantle silicates; often connected to silicate melts associated with clinopyroxenes, amphiboles, and occasionally orthopyroxenes (Fig. 2I). Again, these sulfides occur mainly in the protogranular/porphyroclastic xenoliths.

All four types of sulfide assemblage occur in the protogranular/porphyroclastic xenoliths, where the Type-i and Type-e sulfides (Fig. 2A–E) are larger than the Type-f and Type-b assemblages (Fig. 2H and 2I). The equigranular xenoliths and recrystallized xenoliths all contain the Type-i, Type-e, and Type-f sulfide assemblages, but lack the Type-b sulfides. In these xenoliths the sulfides are small (Fig. 2F) and their abundances are very low. Amphiboles in the metasomatized xenolith contain Type-e and Type-f sulfides (Fig. 2G). Using the classification of Roedder (1984), the Type-e sulfide blebs are clearly primary inclusions. Because the Type-i sulfides have identical compositions and textures (but different distribution), they are also assumed to be primary. Similarly, the Type-f sulfides are clearly secondary inclusions and, by analogy, the Type-b are also assumed to be secondary, based on compositions and textures that are similar to the Type-f sulfides.

5. SULFIDE ASSEMBLAGE MINERALOGY

Sulfide assemblages consist of pentlandite (Pn), chalcopyrite (Cp), pyrrhotite-like monosulfide solid solution (MSS), violarite (Vi), and rarely pyrrhotite (Po), without primary magnetite or secondary iron hydroxides. Except for sulfides in the metasomatized xenoliths, Pn is the predominant phase in the sulfide assemblage. However, Pn occurs only rarely as a monomineralic grain.

A summary of the distribution of sulfide types and assemblages in the NGVF xenoliths is shown in Table 1. In the protogranular/porphyroclastic xenoliths, both Type-i and Type-e sulfide assemblages are composed mostly of one or the other of two different phase assemblages: (1) Cp + Pn (+Vi) (Fig. 2B to D); and (2) MSS + Cp + Pn (+Vi) (Fig. 2A and 2E). The Vi phase, which occurs at the edges of the sulfide grains associated with Pn, shows fractures (Fig. 2A, 2B, and 2D). MSS sometimes exhibits a flame-like linear exsolution of Pn (Fig. 2E). Type-f and Type-b sulfide grains in the protogranular/porphyroclastic xenoliths usually appear to be monomineralic phases and they are indistinguishable mineralogically from the sulfide phases of Type-i or Type-e sulfide assemblages. However, the small grain size of Type-f and Type-b inclusions precludes a more detailed examination (Table 1).

Sulfide assemblages in both the equigranular and the recrystallized xenoliths show the same mineralogy. Type-i and Type-e sulfide assemblages are composed mostly of Pn + MSS (Fig. 2F). Assemblages composed of Pn ± Cp ± Po appear only occasionally. Type-f sulfide grains appear to be monomineralic phases of MSS, or, rarely, Pn and Cp (Table 1).

In the metasomatized xenoliths the sulfides (Type-e and Type-f) are monomineralic grains composed of MSS (Table 1). Type-i and Type-b sulfides are not present.

6. SULFIDE ASSEMBLAGE CHEMISTRY

The chemical composition of Pn in the Type-e and Type-i sulfide grains shows a wide range in Fe/Ni ratios (Fig. 4). However, Pn in the protogranular/porphyroclastic xenoliths has considerably higher Ni + Co content than Pn from the equigranular and recrystallized xenoliths (Fig. 3). The concentration of Cu in Pn is always less than 1 wt%. Pentlandite in the protogranular/porphyroclastic xenoliths shows the lowest Fe/Ni ratios, whereas Pn in the recrystallized xenoliths displays the highest values (Fig. 4).

MSS shows a wide compositional range which varies continuously towards Po composition (Table 2 and Fig. 3). MSS containing less than around 5 wt% Ni is referred to here as Po. Accordingly, only a few Po phases from the equigranular and the recrystallized xenoliths have been identified. The S content in the MSS is closer to the composition of Fe_9S_{10}-type Po than that of Fe_7S_8-type Po (Fig. 5).

Chalcopyrite is slightly Cu-deficient, with respect to stoichiometric $CuFeS_2$, in all of the NGVF ultramafic xenoliths (Fig. 6). Chalcopyrite contains Ni ranging from 0.2–2 wt%.

The Vi compositions are slightly sulfur-deficient and lie just below the violarite-polydymite solid solution join (Fig. 7) and range from polydymite-rich solid-solution (Ni ≈ 50.9 wt%; Co ≈ 8.8 wt%; Fe ≈ 4.8 wt%) to violarite-rich solid-solution (Ni ≈ 43.7 wt%; Co ≈ 0.9 wt%; Fe ≈ 16.6 wt%).

Compositions of Pn, MSS, and Cp reported here are consistent with compositions of these same phases in the well-studied alpine massif peridotites from the northern Pyrenees, France (Lorand, 1989a).

7. DISCUSSION

7.1. Possible Origins of the Bulk Sulfide Compositions

7.1.1. Desulfidation

Based on exhaustive studies of sulfide assemblages in upper mantle lherzolite xenoliths from France and alpine massif peridotites from the Mediterranean region, Lorand (1990) concluded that upper mantle peridotite xenoliths derived from subcontinental lithospheric mantle cannot be used to infer the sulfur content of the upper mantle due to desulfidation during partial melting events in the mantle. Lorand (1990) further stated that sulfur may also be lost during weathering of the mantle-derived sulfide assemblages at the earth's surface. This latter interpretation appears to be valid for the French Massif Central xenoliths based on the remarkable difference in chemistry between interstitial sulfides (Type-i) and primary, enclosed sulfides (Type-e) (Lorand and Conquéré, 1983). In contrast to this, detailed petrographic studies of sulfides from Nógrád-Gömör Volcanic Field xenoliths show no evidence for a widespread weathering process. The lone exception is the replacement of pentlandite by violarite in the protogranular/porphyroclastic xenoliths, resulting in Fe and S loss (Figs. 3 and 7). This alteration effect can be accounted

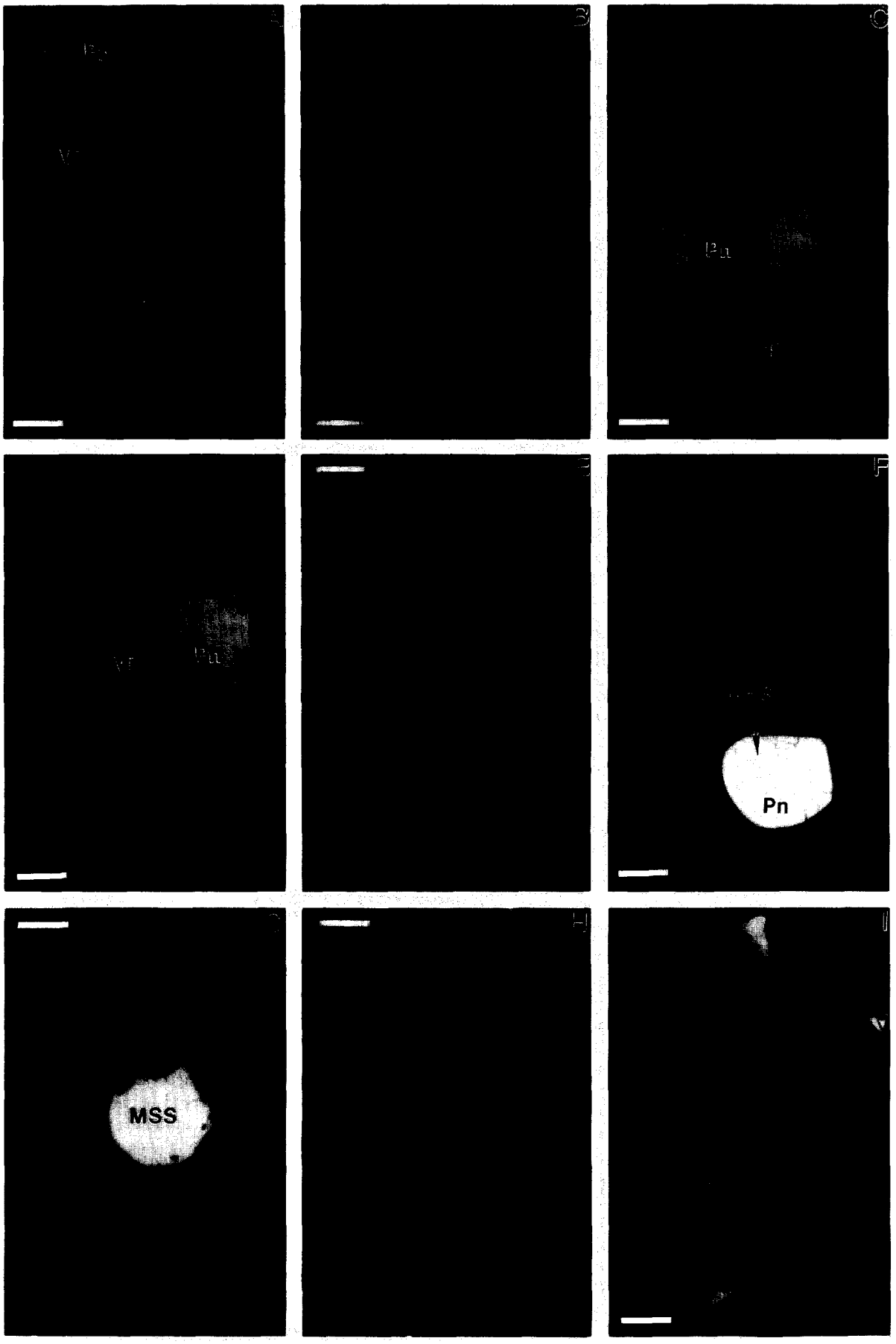
A
B
C
D
E
F
Pn
G
MSS
H
I

for when calculating the original sulfide composition if pentlandite is used in place of its alteration phase violarite in the calculation. Weathering effects described by Lorand (1990) are, therefore, apparently not universal because compositional differences between Type-i and Type-e sulfide assemblages have not been observed in Nógrád-Gömör Volcanic Field nodules (Fig. 3), nor in the well-known Kilbourne Hole xenoliths studied by Dromgoole and Pasteris (1987).

Dromgoole and Pasteris (1987) suggested that desulfidation of the French Massif Central nodules studied by Lorand and Conquéré (1983) might have occurred during mantle metasomatism (i.e., formation of amphiboles). This interpretation was based on the fact that French Massif Central nodules (Lorand and Conquéré, 1983) which show desulfidation are also rich in amphiboles. Conversely, Kilbourne Hole xenoliths (Dromgoole and Pasteris, 1987) that show no evidence of metasomatism (do not contain amphiboles) show no evidence of desulfidation. In the Nógrád-Gömör Volcanic Field xenoliths, nodules with the highest sulfide abundances (~0.5 vol%) also have the highest amphibole content (3–4 vol%). Similarly, xenoliths showing the lowest sulfide abundances (<0.02 vol%) contain no amphiboles (Szabó and Taylor, 1994). These observations would appear to contradict the suggestion of Dromgoole and Pasteris (1987) that desulfidation might be a result of metasomatism because it is clear that sulfides in the metasomatized xenolith (NFL11) show an unambiguous genetic relationship to the metasomatic event. As an alternative, we suggest that Dromgoole and Pasteris (1987) may be correct, but that the sulfur content is also affected by deformation and recrystallization of the xenoliths. These latter processes may, in some cases, be more important than the metasomatism. For example, the least deformed protogranular/porphyroclastic xenoliths have the highest sulfide abundances (~0.5 vol%), whereas the more deformed equigranular and recrystallized xenoliths have the lowest sulfide contents (less than 0.02 vol%). This correlation is consistent with desulfidation during mantle metasomatism, as proposed by Dromgoole and Pasteris (1987), but suggests that deformation and recrystallization are also important and may not represent isochemical processes (e.g., Downes, 1990; Szabó and Taylor, 1994).

The abundance of sulfides in the NGVF protogranular/porphyroclastic xenoliths is as high as sulfide abundances reported for clinopyroxenite xenoliths (Dromgoole and Pasteris, 1987; Anderson et al., 1987) and pyroxenite layers in alpine peridotite (Lorand, 1989b). Furthermore, sample NMS10 (one of the NGVF protogranular/porphyroclastic xenoliths) probably is a pyroxenite-derived websterite showing typical low Mg and Cr (but not Ni) and high Ca, Al, Na, and Si contents (Szabó and Taylor, 1994). Unfortunately, there is no evidence to indicate that the other two NGVF protogranular/porphyroclastic xenoliths (NMS09 and NMS16) have a similar origin, except that both show a high sulfide content similar to sample NMS10. Thus, it cannot be ruled out that NGVF protogranular/porphyroclastic samples represent old pyroxenite-derived layers of the mantle, produced during a partial melting event, and which were later involved in additional mantle processes (partial melting, deformation, recrystallization, metasomatism, etc.).

Table 1. Distribution of sulfide types and assemblages occurring in different Cr-diopside peridotite xenolith types from the Nógrád-Gömör Volcanic Field.

Sample	Type-i	Type-e	Type-f	Type-b
Protogranular/ porphyroclastic	Pn (+ Vi) +Cp Pn (+ Vi) +Cp + MSS	Pn (+ Vi) +Cp Pn (+ Vi) +Cp + MSS	Pn, Cp, MSS, Vi	Pn, Cp, MSS, Vi
Equigranular	Pn + MSS Pn ± Cp ± Po	Pn + MSS Pn ± Cp ± Po	Pn, MSS, Cp	n.p.
Recrystallized	Pn + MSS Pn ± Cp ± Po	Pn + MSS Pn ± Cp ± Po	Pn, MSS, Cp,	n.p.
Metasomatized	n.p.	MSS	MSS	n.p.

Pn = Pentlandite; Vi = Violarite; Cp = Chalcopyrite; MSS = Monosulfide Solid Solution; Po = Pyrrhotite.
n.p. = not present

7.1.2. *Fe loss*

Based on experimental data of Naldrett (1989a), Eggler and Lorand (1993) proposed that the Fe_3O_4 component may be lost from a high-temperature sulfide melt during recrystallization of MSS in equilibrium with mantle minerals. In the Nógrád-Gömör Volcanic Field, spinels in the metasomatized and recrystallized xenoliths have the highest Fe_3O_4 compo-

FIG. 2. Photomicrographs of textural relations of sulfide assemblages in Cr-diopside xenoliths from the NGVF. (Scale bar equals 10 microns, except in photos F, G, H, and I where scale bar equals 20 microns. Photos were taken under plane polarized reflected light using oil immersion.) (A) Type-e sulfide assemblage with fretted rim and numerous satellites in olivine. Sulfide inclusion is composed of chalcopyrite (Cp), monosulfide solid solution (MSS), pentlandite (Pn), and violarite (Vi). Lherzolite from protogranular/porphyroclastic xenoliths. (B) Type-i sulfide assemblage composed of chalcopyrite (Cp), pentlandite (Pn), and violarite (Vi). Websterite from protogranular/porphyroclastic xenoliths. (C) Type-i sulfide assemblage with linear borders. Sulfide phases are chalcopyrite (Cp), pentlandite (Pn), and violarite (Vi). Websterite from protogranular/porphyroclastic xenoliths. (D) Type-e sulfide assemblage (in olivine) composed of chalcopyrite (Cp), pentlandite (Pn), and violarite (Vi). Lherzolite from protogranular/porphyroclastic xenoliths. (E) Type-e sulfide assemblage composed of chalcopyrite (Cp), monosulfide solid solution (MSS), and pentlandite (Pn). MSS exhibits flame-like exsolution of Pn. Lherzolite from protogranular/porphyroclastic xenoliths. (F) Spherical-shaped Type-e sulfide assemblage (in olivine) in composed of monosulfide solid solution (MSS) and pentlandite (Pn). Lherzolite from recrystallized xenoliths. (G) Monomineralic Type-e and Type-f sulfide inclusions (in amphibole) composed of monosulfide solid solution (MSS). Amphibole peridotite from metasomatized xenolith. (H) Type-f sulfide inclusions along healed fracture in clinopyroxene. Lherzolite from protogranular/porphyroclastic xenoliths. (I) Type-b sulfide inclusions associated with silicate melt inclusions in clinopyroxene. Lherzolite from protogranular/porphyroclastic xenoliths.

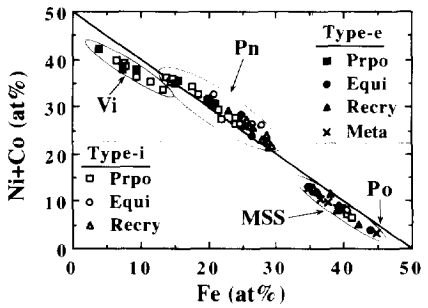

FIG. 3. Plot of Fe (at%) vs. Ni + Co (at%) showing compositional ranges of pentlandite (Pn), monosulfide solid solution (MSS), violarite (Vi) and pyrrhotite (Po) in Type-e and Type-i sulfide assemblages. Prpo = protogranular/porphyroclastic xenoliths, Equi = equigranular xenoliths, Recry = recrystallized xenoliths, and Meta = metasomatized xenolith.

nent, spinels in the protogranular/porphyroclastic xenoliths have the lowest Fe_3O_4 component, and the equigranular xenoliths have intermediate values (Fig. 8) (Szabó and Taylor, 1994). These observations suggest that some Fe from the sulfide assemblages might have been incorporated into spinel as Fe_3O_4 in the recrystallized and, probably, in the equigranular xenoliths. This interpretation is consistent with the reduced sulfide-abundances of these two xenolith groups, and is consistent with desulfidation during deformation and recrystallization discussed above.

Iron loss as an explanation for the observed sulfide contents is also consistent with calculated sulfur fugacities of the melts, calculated using equations in Eggler and Lorand (1993). The metasomatized and recrystallized xenoliths show the highest sulfur fugacity, whereas the protogranular/porphyroclastic xenoliths have the lowest fS_2 (Fig. 8). The equigranular xenoliths have intermediate fS_2 values. This suggests that recrystallization and metasomatism occurred at relatively high sulfur fugacities. Oxygen fugacity variation is also consistent with this interpretation (Szabó and Taylor, 1994).

7.1.3. Sulfide-silicate equilibria

A mantle origin for the sulfide compositions can also be tested by comparing Ni and Fe contents of sulfides and coexisting olivines. Experimental values for the Ni/Fe exchange between olivine and sulfide pairs ($NiSi_{1/2}O_{2,ol}$ + FeS_{sulf} = NiS_{sulf} + $FeSi_{1/2}O_{2,ol}$) range from 22–41 (Fleet and Stone, 1990). Bulk compositions of coexisting sulfides and olivines in five xenoliths (Table 3) from the Nógrád-Gömör Volcanic Field are consistent with equilibration at high temperature according to the partition coefficients (K_{D3}) presented by Fleet and Stone (1990, and references therein). These five xenoliths include all three of the protogranular/porphyroclastic xenoliths ($25 < K_{D3} < 42$), one equigranular xenolith (NBN54; $K_{D3} = 23$), and one recrystallized xenolith (NBN51; $K_{D3} = 23$). The remainder of the xenoliths show calculated K_{D3} values for olivine-bulk sulfide pairs in the range from 3–16 (Table 3). Elevated FeS contents of sulfides with the low K_{D3} values (Table 3) are thought to reflect introduction of Fe from host alkaline lavas. This must have occurred later than the deformation, recrystallization, and metasomatic processes which had earlier modified the compositions of sulfides. Based on our analyses, it appears that textures and compositions of sulfides in the subcontinental lithospheric mantle are more sensitive to changes in pressure-temperature conditions, compared to silicates, resulting in heterogeneous sulfide compositions and distribution within mantle material.

7.2. Petrogenesis of Sulfide Assemblages in the NGVF Xenoliths

Petrographic and chemical characteristics of sulfides in upper mantle xenoliths are consistent with their origin as an immiscible phase formed during partial melting (e.g., Bishop et al., 1975; De Waal and Calk, 1975; Dromgoole and Pasteris, 1987). Other workers (e.g., Irving, 1980), however, have also suggested an origin by metasomatic fluid infiltration of the lithospheric mantle.

In the protogranular/porphyroclastic, equigranular, and recrystallized xenoliths, the distribution of sulfide inclusions in the mantle silicates (Type-e; Fig. 2F) unambiguously prove that these sulfides existed prior to deformation. Triple junctions among interstitial sulfides (Type-i) and mantle silicates (Fig. 2C) also suggest that sulfides existed prior to recrystallization of the mantle. These textural signatures are similar to those reported for sulfide assemblages from upper mantle xenoliths from other locations (Mitchell and Keays, 1981; Lorand and Conquéré, 1983; Dromgoole and Pasteris, 1987) and from alpine massif peridotites (e.g., Lorand, 1989a). Consequently, there is no question that the sulfides in the protogranular/porphyroclastic, equigranular, and recrystallized xenoliths originated from an immiscible Fe-Ni-Cu sulfide liquid. This sulfide liquid was trapped in the residual mantle during partial melting event(s), similar to the proposed origin of sulfides in other peridotite xenoliths and alpine massif peridotites from around the world. Later subsolidus reactions yielded Pn, Cp, and MSS.

Rounded MSS blebs (Fig. 2G) showing a geometry typical of sulfide liquid with a minimum surface area (Skinner and Peck, 1969) occur only within metasomatic amphiboles in the strongly metasomatized xenolith (NFL11). This geometry and occurrence suggests a metasomatism-related origin for these monomineralic MSS grains. Alternatively, however, it cannot be ruled out that some sulfides were present before the metasomatic fluid invasion. If this scenario is true then the

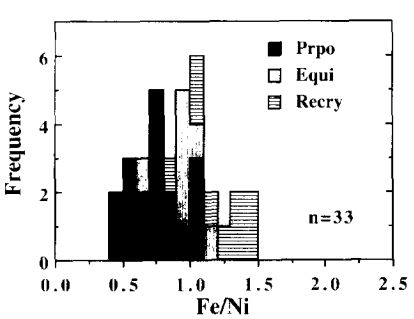

FIG. 4. Histogram showing Fe/Ni atomic ratios of pentlandite from the Type-e and Type-i sulfide assemblages. For abbreviations see Fig. 3.

Table 2. Representative analyses of sulfide phases (wt%) in Type-i, Type-e, Type-f, and Type-b sulfides from the NGVF upper mantle xenoliths.

Type	Type-i	Type-i	Type-i	Type-i	Type-i	Type-i	Type-e	Type-e	Type-e	Type-e	Type-f
Mineral	Pn	Pn	Cp	MSS	Vi	Vi	Pn	Pn	Vi	Vi	Pn
Xenolith	Prpo	Prpo	Prpo	Prpo	Prpo	Prpo	Prpo	Prpo	Prpo	Prpo	Prpo
S	35.1	35.4	34.3	38.2	38.4	38.0	34.6	34.2	39.4	38.3	34.6
Fe	29.9	17.1	31.2	51.6	7.9	9.5	30.9	19.0	9.3	9.2	28.4
Ni	33.7	45.7	0.2	8.3	44.7	49.8	33.6	44.0	49.1	50.9	34.7
Co	1.0	1.5	0.3	1.4	7.9	1.8	1.0	1.8	1.4	1.1	1.5
Cu	0.4	0.2	33.5	0.3	0.3	0.4	0.1	0.5	0.4	0.2	0.4
Total	100.1	99.9	99.5	99.8	99.2	99.5	100.2	99.5	99.6	99.7	99.6

Type	Type-f	Type-b	Type-i	Type-i	Type-i	Type-e	Type-e	Type-e	Type-e	Type-e	Type-f
Mineral	Vi	Pn	Pn	Pn	MSS	Po	Pn	MSS	Cp	MSS	MSS
Xenolith	Prpo	Prpo	Recry	Equi	Recry	Equi	Equi	Recry	Equi	Meta	Meta
S	38.5	36.8	35.0	32.6	37.9	38.3	32.7	38.1	34.5	38.4	38.4
Fe	3.7	22.9	35.1	25.4	50.0	56.2	30.4	46.3	31.4	46.8	45.3
Ni	52.7	37.4	29.5	42.1	11.5	4.9	36.3	15.2	0.3	13.4	14.5
Co	2.5	1.5	0.4	0.2	0.5	0.3	0.5	0.5	0.1	0.5	0.3
Cu	0.6	0.9	0.2	0.2	0.1	0.1	0.3	0.1	33.3	0.3	1.0
Total	98.0	99.5	100.2	100.5	100.0	99.8	100.2	100.2	99.6	99.4	99.5

Pn = Pentlandite; Cp = Chalcopyrite; MSS = Monosulfide Solid Solution; Po = Pyrrhotite; Vi = Violarite
Prpo = Protogranular/porphyroclastic xenoliths from NMS locality;
Equi = Equigranular xenoliths from NBN locality;
Recry = Recrystallized xenoliths from NBN locality;
Meta = Metasomatized xenolith (= amphibole peridotite) from NFL locality

MSS blebs represent the reaction product between earlier sulfides and the metasomatic agent.

7.3. Sulfide Assemblage Crystallization and Subsolidus History

Unmodified bulk sulfide compositions can be used to assess the crystallization and subsolidus history of the sulfide assemblages within upper mantle peridotites. The experimentally determined and well-characterized ternary sulfide systems, Fe-Ni-S and Cu-Fe-S, and the quaternary Fe-Cu-Ni-S system (Yund and Kullerud, 1966; Naldrett et al., 1967; Craig and Kullerud, 1969; Kullerud et al., 1969; Misra and Fleet, 1973; Fleet and Pan, 1994) have been applied in numerous studies which have addressed the origin of sulfide assemblages in upper mantle xenoliths (e.g., De Waal and Calk, 1975; Lorand and Conquéré, 1983; Dromgoole and Pasteris, 1987).

Based on the calculated bulk compositions of sulfides in the NGVF xenoliths (Table 3), the assumed original compositions fall into the range of a single MSS (Kullerud et al., 1969) (Fig. 9) which starts to crystallize at 1150°C and 15 kbar pressure (Ryhzenko and Kennedy, 1973). Volatiles such as CO_2, CO, H_2O, and H_2 and dissolved FeO_x can lower the crystallization temperatures if they are present in the sulfide system (Naldrett, 1969; Anderson et al., 1987). However, because primary magnetite and CO_2 fluid inclusions are not associated with Type-e and Type-i sulfide assemblages in the NGVF xenoliths, we ignore the effect of volatiles and FeO_x on phase equilibria in these sulfide systems.

As shown on Fig. 9, bulk sulfide compositions in the metasomatized, the equigranular, and the recrystallized xenoliths are consistent with those in ultramafic xenoliths from the Kilbourne Hole, southwestern U.S.A. (Dromgoole and Pasteris, 1987) and Massif Central, France (Lorand and Conquéré, 1983; Eggler and Lorand, 1993). In contrast, sulfides in the protogranular/porphyroclastic xenoliths show uncommon Cu, Ni (+Co) enrichment and depletion in Fe (see also Table 3) compared to those in other ultramafic xenoliths from the NGVF, Kilbourne Hole (Dromgoole and Pasteris, 1987), and Massif Central (Lorand and Conquéré, 1983; Eggler and Lor-

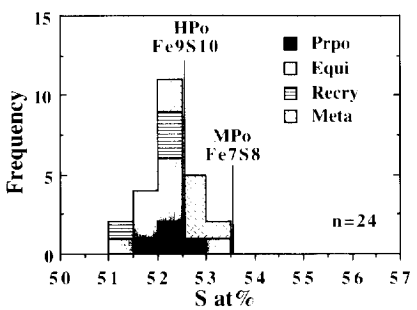

FIG. 5. Histogram showing sulfur content (at%) of monosulfide solid solution from the Type-e and Type-i sulfide assemblages. HPo represents hexagonal pyrrhotite; MPo represents monoclinic pyrrhotite. For other abbreviations see Fig. 3.

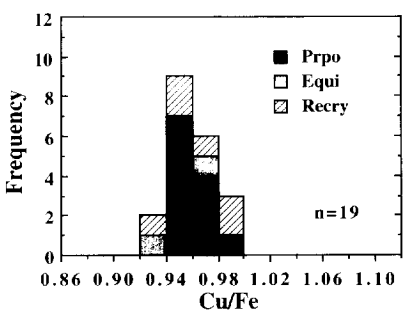

FIG. 6. Histogram showing Cu/Fe atomic ratio of chalcopyrite from the Type-e and Type-i sulfide assemblages. For abbreviations see Fig. 3.

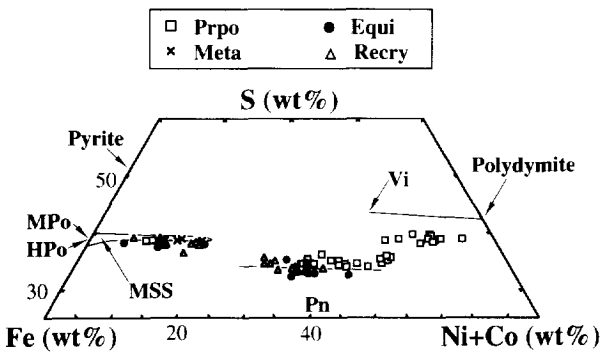

FIG. 7. Compositions of pentlandite (Pn), monosulfide solid solution (MSS), and violarite (Vi) in Type-e and Type-i sulfide assemblages from the NGVF xenoliths. Compositional ranges of MSS, Pn, Vi-Polydymite taken from Kullerud et al. (1969). For abbreviations see Fig. 3 and 5.

and, 1993). All these characteristics combined suggest that the sulfides in the protogranular/porphyroclastic xenoliths represent a high-temperature mixture of an MSS and a coexisting Cu-Ni-rich liquid (Craig and Kullerud, 1969), as shown on Fig. 10. In this diagram the bulk sulfide compositions from the protogranular/porphyroclastic xenoliths occupy the two-phase field of the MSS + Ni-Cu-rich liquid (those from the equigranular and recrystallized xenoliths again plot in the MSS field). It is possible that before the mantle (from which the protogranular/porphyroclastic xenoliths originated) cooled to a moderate equilibrium temperature (ranging from 920–960°C; Szabó and Taylor, 1994) a Cu-Ni-rich liquid was dispersed interstitially to and/or as an enclosed phase in silicates. This may have occurred, for instance, during the high-temperature plastic deformation event. Therefore, we believe that the Cu-Ni-rich liquid is a high-temperature precursor of the Type-e and Type-i sulfide assemblages composed of Cp + Pn (+Vi) phases (Fig. 2B–D).

High-temperature MSS can contain about 7 wt% Cu at 935°C (Kullerud et al., 1969; Cabri, 1973), which begins to exsolve at 900°C (Dutrizac, 1976) as a Cu-rich intermediate solid solution (ISS). On cooling, ISS should continue to exsolve from the MSS until some other phase change intervenes, in this case the appearance of Pn. In general, Pn starts to crystallize at 500–600°C (Kullerud, 1963; Naldrett, 1989b), leaving behind a Ni-reduced MSS (Fig. 7). However, the flame-like exsolution textures of Pn in some sulfide assemblages (Fig. 2E and 2G) suggest a very low (<150°C) re-equilibration temperature according to several other occurrences (e.g., Durazzo and Taylor, 1982; Kelly and Vaughan, 1983). Estimation of the subsolidus re-equilibration temperature from the extent of Ni substitution in MSS (after Dromgoole and Pasteris, 1987) (Fig. 7) also implies a blocking temperature less than 200°C. Thus, it is plausible that the high-temperature MSS occurring in the upper mantle (from which the protogranular/porphyroclastic xenoliths are derived) could be a precursor of the Type-e and Type-i sulfide assemblages composed of MSS + Cp + Pn (+Vi) phases (Fig. 2A and 2E).

As described previously, Vi occurs only in the protogranular/porphyroclastic xenoliths (Fig. 2A–D). This phase can form by alteration of Pn below 200°C (e.g., Kullerud et al., 1969; Craig, 1973), or can exsolve from a Ni-MSS at moderate (~450°C) temperatures (e.g., Craig, 1971; Naldrett, 1989b). Considering that Vi in the protogranular/porphyroclastic xenoliths shows a strong association with Pn, we believe that Vi in the protogranular/porphyroclastic xenoliths was formed by alteration of Pn. Nevertheless, it should be noted that, we have not observed textural features such as porous surfaces or Pn relicts within Vi (e.g., Craig and Higgins, 1975) which are indicative of secondary Vi. However, Vi in our samples is sulfur-deficient (or metal-enriched) (Fig. 7) which has been reported for Vi for several other locations (e.g., Desborough and Czamanske, 1973; Craig and Scott, 1974).

Sulfide assemblages (Pn + MSS and Pn ± Cp ± Po) in the equigranular and recrystallized xenoliths probably had a simplified crystallization history compared to those in the protogranular/porphyroclastic nodules described above. The bulk sulfide compositions of the equigranular and recrystallized xenoliths do not show the extremely high Ni (and Co) and/or Cu contents discussed above (Table 3). These data suggest that MSS was the only sulfide-bearing phase present in the xenoliths in the mantle. However, the calculated composition of MSS may not represent the original composition. As discussed previously, sulfide compositions in the majority of the equigranular and recrystallized xenoliths changed during deformation and recrystallization and transport to the surface by the alkaline basaltic lavas. The minimum blocking temperature or subsolidus re-equilibration temperature estimated from the extent of Ni substitution in MSS is about 250°C (after Dromgoole and Pasteris, 1987) (Fig. 9).

7.4. Formation of Type-f and Type-b Sulfide Inclusions

Many Type-f and Type-b sulfide assemblages (i.e., secondary inclusions) occurring in the protogranular/porphyroclastic xenoliths (Fig. 2H and 2I) show chemical compositions similar to those of phases in the Type-e and Type-i sulfide assemblages. This suggests that the Type-e and Type-i sulfides are a possible source of the secondary sulfide inclusions. Thus, the question that must be considered is when and how these sulfide inclusions with the same chemistry as the Type-e and Type-i sulfide assemblages could have formed.

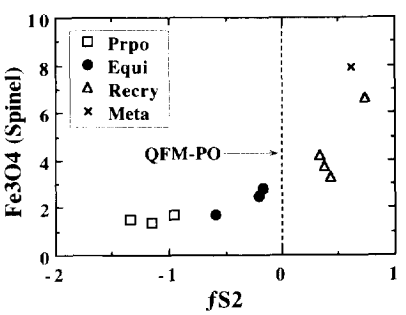

FIG. 8. Calculated $\log fS_2$ of bulk sulfide assemblages from NGVF xenoliths (relative to QFM-PO) plotted against Fe_3O_4 component in the coexisting spinel. Sulfur fugacity was computed using the equation of Eggler and Lorand (1993), and the Fe_3O_4 component of spinel is from Szabó and Taylor (1994). For abbreviation see Fig. 3.

Table 3. Bulk sulfide composition and Ni/Fe partitioning data for bulk sulfide composition/coexisting olivine from NGVF xenoliths

Sample	S wt%	Fe wt%	Ni wt%	Co wt%	Cu wt%	Bulk sulfide FeS (mol%)	Bulk sulfide NiS (mol%)	Coexisting olivine° Ni2SiO4 (mol%)	Coexisting olivine° Fe2SiO4 (mol%)	KD3•
Protogranular/porphyroclastic xenoliths										
NMS09	34.5	25.7	31.0	1.1	7.9	40.7	46.7	0.35	10.1	33
NMS10	34.8	27.8	30.8	1.0	5.5	44.2	46.6	0.35	13.9	42
NMS16	35.5	29.9	26.4	1.4	6.9	47.9	40.3	0.35	10.2	25
Equigranular xenoliths										
NBN27	38.1	54.9	6.0	0.3	0.7	89.3	9.23	0.35	10.4	3
NBN30	38.0	44.3	16.9	0.5	0.3	72.5	26.3	0.35	9.36	10
NBN54	35.8	36.5	27.4	0.3	0.1	58.0	41.5	0.30	9.58	23
Recrystallized xenoliths										
NBN15	37.7	48.1	11.1	0.5	2.6	78.4	17.2	0.30	9.24	7
NBN22	37.0	42.7	19.6	0.4	0.2	68.9	30.1	0.30	10.7	16
NBN23	36.5	42.6	17.4	0.4	3.0	68.5	26.6	0.35	8.67	10
NBN51	35.5	36.6	26.3	0.4	1.2	58.1	39.6	0.30	10.1	23
Metasomatized xenolith										
NFL11	38.5	48.3	12.3	0.7	0.3	79.4	19.2	0.25	13.2	13

° Data (SZABÓ and TAYLOR, 1994)
• KD3 = XNiS * XFe2SiO4 / XFeS * XNi2SiO4 (FLEET and STONE, 1990)

An obvious approach to answer this question is to test the effect of the entrainment of the upper mantle xenoliths into the host lavas on sulfide behavior. This process would produce a heating event in the upper mantle xenoliths and could cause partial melting of the mantle material, including the sulfides. Two-pyroxene geothermometry (Brey and Köhler, 1990) gives temperatures ranging from 920–960°C for the protogranular/porphyroclastic xenoliths (Szabó and Taylor, 1994). This temperature range is indicative of the mantle material, including the sulfides, prior to ascent in the host lavas. Accordingly, the sulfide material in the protogranular/porphyroclastic xenoliths had to be a solid MSS existing with Ni- and Cu-rich liquid at the moment of entrainment of the xenoliths. The elevated temperature of the ascending host lavas could have been high enough to melt the MSS, which melts at approximately 1040–1095°C at 10 kbar (Hsieh et al., 1987; Ryzhenko and Kennedy, 1973). Thus, the composition of the sulfide-forming melt was very similar to that of the parental melt of MSS and Ni-Cu-rich liquid. The sulfide melt migrated along fractures and grain borders which also show the presence of CO_2 and silicate melt (Szabó et al., 1994). Following entrainment and heating, the sulfide melt cooled down along the same subsolidus path as that of the Type-e and Type-i sulfide assemblages discussed previously. During cooling, the sulfide melt, silicate melt, and CO_2 fluid remained as immiscible phases (Kogarko and Pacheco, 1994) because the temperature was too low to form a single miscible CO_2- and sulfide-bearing melt (Anderson et al., 1987). Alternatively, it is possible that the various fluids migrated along the

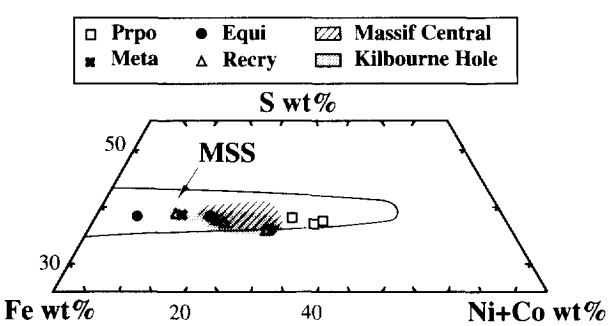

FIG. 9. Bulk composition of sulfides in NGVF xenoliths plotted in the Fe-Ni-S ternary system. The stability field of MSS at 1,000°C (Kullerud et al., 1969) is shown for comparison. Also shown are measured compositions of sulfides in xenoliths from the Massif Central, France (Eggler and Lorand, 1993) and Kilbourne Hole, southwestern USA (Dromgoole and Pasteris, 1987). For abbreviations see Fig. 3.

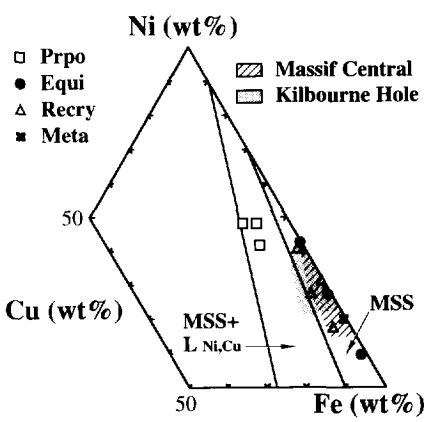

FIG. 10. Bulk compositions of sulfides from NGVF xenoliths plotted on Fe-Ni-Cu projection in the Fe-Ni-Cu-S quaternary system. The MSS and MSS + Ni-Cu-rich liquid ($L_{Ni,Cu}$) fields at 1,000°C (Craig and Kullerud, 1969) are shown for comparison. Also shown are measured compositions of sulfides in xenoliths from the Massif Central, France (Eggler and Lorand, 1993) and Kilbourne Hole, southwestern U.S.A. (Dromgoole and Pasteris, 1987). For other abbreviations see Fig. 3.

same fractures at different temperatures (following immiscibility).

7.5. Formation of the Type-e and Type-f Sulfide Inclusions in the Metasomatized Xenolith

The Type-e monomineralic MSS sulfide blebs (Fig. 2G, Table 2) representing primary inclusions occur in metasomatically-derived amphiboles (Szabó and Taylor, 1994). Amphiboles formed from mantle-derived andesitic liquid (Szabó et al., 1994) within the sub-continental lithospheric mantle beneath the Nógrád-Gömör Volcanic Field. This metasomatic agent contained sufficient sulfide to reach sulfide saturation as a result of a small temperature decrease. This origin for sulfide blebs is common, and a similar origin has been described for sulfides in clinopyroxene megacrysts from alkali basalts around the world (Anderson et al., 1987) and in alkali basalt-derived amphibole-rich veins from alpine massif peridotites, France (Lorand, 1989c).

Formation of the Type-f sulfide inclusions in the vicinity of Type-e blebs might be attributed to partial decrepitation, similar to that often observed around CO_2 fluid inclusions in mantle rocks (Roedder, 1984). It is probable that partial decrepitation took place when the Type-e sulfide inclusions were partly melted by the heating effect of the host basaltic lavas. Anderson et al. (1987) proposed a similar explanation for the formation of sulfide halos and apophyses around sulfide inclusions in clinopyroxene megacrysts.

8. CONCLUSIONS

Petrographic observations and microanalysis of sulfide inclusions in xenoliths from the Nógrád-Gömör Volcanic Field reveal a complex crystallization and deformation history in the underlying mantle. Significant differences in chemistry are not observed between primary (Type-e and Type-i) and secondary (Type-b and Type-f) sulfide assemblages, which is consistent with the origin of secondary sulfides by remobilization of the primary sulfide phases. This process probably occurred during entrainment of xenoliths into the host alkali basalts.

Differences in mineralogy and chemistry between enclosed (Type-e) and interstitial (Type-i) sulfide assemblages from the Nógrád-Gömör Volcanic Field xenoliths were not observed. This suggests that both types of primary sulfides underwent the same mantle processes. Sulfides in these xenoliths are interpreted to have formed from immiscible sulfide liquid trapped during (or after) partial melting of the mantle.

Sulfide assemblages in the equigranular xenoliths and recrystallized xenoliths are indistinguishable texturally and chemically. However, they differ significantly from sulfide assemblages in the protogranular/porphyroclastic xenoliths where sulfide assemblages are more abundant and richer in Ni (+Co) and Cu than those in both former xenolith groups. This reflects the important link between relatively recent deformation and recrystallization and sulfide chemistry. Note, however, that the observed differences in sulfide chemistry might reflect original compositional variations in the mantle. Specifically, protogranular/porphyroclastic xenoliths might represent older pyroxenites which originated during partial melting in the mantle.

Metasomatism was responsible for the formation of sulfide components in metasomatized xenoliths. However, those sulfides occurring in the metasomatized xenolith show a very simple texture and chemistry compared to sulfides in the other Nógrád-Gömör Volcanic Field xenolith groups.

Acknowledgments—Thanks are due to J. R. Craig, L. A. Taylor, H. E. Belkin, and R. J. Tracy for helpful discussions. Detailed comments on an earlier version of this manuscript by T. A. Abrajano and an anonymous reviewer improved the manuscript significantly. We offer special thanks to Paul Barton, Jr. for many helpful and insightful comments concerning sulfide petrology and geochemistry. We also thank J. A. Mavrogenes and T. N. Solberg for technical assistance with the SEM. S. Chaing drafted several of the diagrams.

Editorial handling: D. A. Vanko

REFERENCES

Anderson T., Griffin W. L., and O'Reilly S. Y. (1987) Primary sulphide melt inclusions in mantle-derived megacrysts. *Lithos* **20,** 279–294.

Bishop F. C., Smith J. V., and Dawson J. B. (1975) Pentlandite-magnetite intergrowth in DeBeers spinel lherzolite. *Phys. Chem. Earth* **9,** 323–327.

Brey G. P. and Köhler T. (1990) Geothermobarometry in four-phase lherzolites II. New thermobarometers, and practical assessment of existing thermobarometers. *J. Petrol.* **31,** 1353–1378.

Cabri L. J. (1973) New data on phase relations in the Cu-Fe-S system. *Econ. Geol.* **68,** 443–454.

Craig J. R. (1971) Violarite stability relations. *Amer. Mineral.* **56,** 1303–1311.

Craig J. R. (1973) Pyrite-pentlandite assemblages and other low temperature relations in the Fe-Ni-S system. *Amer. J. Sci.* **273A,** 496–510.

Craig J. R. and Higgins J. B. (1975) Cobalt- and iron-rich violarite from Virginia. *Amer. Mineral.* **60,** 35–38.

Craig J. R. and Kullerud G. (1969) Phase relations in the Cu-Fe-Ni-S system and their applications to magmatic ore deposits. In *Magmatic Ore Deposits* (ed. H. D. B. Wilson); *Econ. Geol. Monogr.* **4,** 343–358.

Craig J. R. and Scott S. D. (1974) Sulfide phase equilibria. *Sulfide Mineral. Min. Soc. Amer. Short Course Notes* **1,** CS1–CS110.

Desborough G. A. and Czamanske G. K. (1973) Sulfides in eclogite nodules from a kimberlite pipe, South Africa, with comments on violarite stoichiometry. *Amer. Mineral.* **58,** 195–202.

De Waal S. A. and Calk L. C. (1975) The sulfides in the garnet pyroxenite xenoliths from Salt Lake crater. Oahu. *J. Petrol.* **16,** 134–153.

Downes H. (1990) Shear zones in the upper mantle—relation between geochemical environment and deformation in mantle peridotites. *Geology* **8,** 374–377.

Dromgoole E. L. and Pasteris J. D. (1987) Interpretation of the sulfide assemblages in a suite of xenoliths from Kilbourne Hole, New Mexico. *Geol. Soc. Amer. Spec. Paper* **215,** 25–46.

Durazzo A. and Taylor L. A. (1982) Exsolution in the mss-pentlandite system: Textural and genetic implications for Ni-sulfide ores. *Mineral. Deposita* **17,** 313–332.

Dutrizac J. E. (1976) Reactions in cubanite and chalcopyrite. *Canadian Mineral.* **14,** 172–181.

Eggler D. H. and Lorand J. P. (1993) Mantle sulfide geobarometry. *Geochim. Cosmochim. Acta* **57,** 2213–2222.

Fleet M. E. and Pan Y. (1994) Fractional crystallization of anhydrous sulfide liquid in the system Fe-Ni-Cu-S, with application to magmatic sulfide deposits. *Geochim. Cosmochim. Acta* **58,** 3360–3377.

Fleet M. E. and Stone W. E. (1990) Nickeliferous sulfides in xenoliths, olivine megacrysts and basaltic glass. *Contrib. Mineral. Petrol.* **105,** 629–636.

Frick C. (1973) The sulfides in griquaite and garnet-peridotite xenoliths in kimberlite. *Contrib. Mineral. Petrol.* **39,** 1–16.

Gedcke D. A., Byars L. G., and Hardy W. H. (1982) ZAP—A Standardless X-ray microanalysis computer program. *Scanning Electron Microsc.* **III,** 981–993.

Hsieh K.-C., Vlach K. C., and Chang Y. A. (1987) The Fe-Ni-S system: I. A thermodynamic analysis of the phase equilibria and calculation of the phase diagram from 1173 to 1623 K. *High Temp. Sci.* **23,** 17–38.

Irving A. J. (1980) Petrology and geochemistry of composite ultramafic xenoliths in alkalic basalts and implications for magmatic processes within the mantle. *Amer. J. Sci.* **280A,** 389–426.

Kelly D. P. and Vaughan D. J. (1983) Pyrrhotine-pentlandite ore textures: a mechanistic approach. *Mineral. Mag.* **47,** 453–463.

Kogarko L. N. and Pacheco A. H. (1994) Mechanism of carbonatized peridotite partial melting. *16th Intl. Miner. Assoc., Abstr.* 208–209.

Kullerud G. (1963) Thermal stability of pentlandite. *Canadian Mineral.* **7,** 353–366.

Kullerud G., Yund R. A., and Mohr G. (1969) Phase relations in the Cu-Fe-S, Cu-Ni-S systems. In *Magmatic Ore Deposits* (ed. H. D. B. Wilson); *Econ. Geol. Monogr.* **4,** 323–343.

Lorand J. P. (1989a) Mineralogy and chemistry of Cu-Fe-Ni sulfides in orogenic-type spinel peridotite bodies from Ariége (Northeastern Pyrenees, France). *Contrib. Mineral. Petrol.* **103,** 335–345.

Lorand J. P. (1989b) Sulfide petrology of spinel and garnet pyroxenite layers from mantle-derived spinel lherzolite massifs of Ariége, northeastern Pyrenees, France. *J. Petrol.* **30,** 987–1015.

Lorand J. P. (1989c) The Cu-Fe-Ni sulfide component of the amphibole-rich veins from the Lherz and Freychinéde spinel peridotite massifs (Northeastern Pyrenees, France): A comparison with mantle-derived megacrysts from alkali basalts. *Lithos* **23,** 281–298.

Lorand J. P. (1990) Are spinel lherzolite xenoliths representative of the abundance of sulfur in the upper mantle? *Geochim. Cosmochim. Acta* **54,** 1487–1492.

Lorand J. P. and Conquéré F. (1983) Contribution á l'étude des sulfures dans les enclaves de lherzolite á spinelle des basaltes alcalins (Massif Central, et Languedoc, France). *Bull. Minéral.* **106,** 585–605.

Meyer H. O. A. and Boctor N. Z. (1975) Sulfide-oxide minerals in eclogite from Stockdale kimberlite, Kansas. *Contrib. Mineral. Petrol.* **52,** 57–68.

Misra K. C. and Fleet M. E. (1973) The chemical compositions of synthetic and natural pentlandite assemblages. *Econ. Geol.* **68,** 518–539.

Mitchell R. H. and Keays R. R. (1981) Abundance and distribution of gold, palladium and iridium in some spinel and garnet lherzolite. Implications for the nature and origin of precious metal-rich intergranular components in the upper mantle. *Geochim. Cosmochim. Acta* **45,** 2425–2445.

Naldrett A. J. (1969) A portion of the system Fe-S-O between 900°C and 1080°C and its applications to sulfide ore magmas. *J. Petrol.* **10,** 171–201.

Naldrett A. J. (1989a) Sulfide melts: Crystallization temperatures, with solubilities in silicate melts, and Fe, Ni, and Cu partitioning between basaltic magmas and olivine. In *Ore Deposition Associated with Magmas* (ed. J. A. Whitney and A. J. Naldrett), pp. 5–20. Soc. Econ. Geologists.

Naldrett A. J. (1989b) Magmatic Sulfide Deposits. *Oxford Monogr. Geol. Geophys.* **14,** 17–38.

Naldrett A. J., Craig J. R., and Kullerud G. (1967) The central portion of the Fe-Ni-S system and its bearing on peridotite exsolution in iron-nickel sulfide ores. *Econ. Geol.* **70,** 824–833.

Roedder E. (1984) Fluid Inclusions. *Rev. Mineral.* **12,** 644.

Ryzenkho B. and Kennedy G. C. (1973) The effect of pressure on the eutectic in the Fe-FeS system. *Amer. J. Sci.* **273,** 803–810.

Skinner B. J. and Peck D. L. (1969) An immiscible sulfide melt from Hawaii. In *Magmatic Ore Deposits* (ed. H. D. B. Wilson); *Econ. Geol. Monogr.* **4,** 310–322.

Szabó Cs. and Taylor L. A. (1991) Mantle xenoliths from alkali basalts in the Nógrád-Gömör region of Hungary and Czechoslovakia. *5th Intl. Kimberlite Conf., Brasilia. Extended abstracts, Spec. Publ.* **2/91,** 401–404.

Szabó Cs. and Taylor L. A. (1994) Mantle petrology and geochemistry beneath the Nógrád-Gömör Volcanic Field, Carpathian-Pannonian Region. *Intl. Geol. Rev.* **36,** 328–258.

Szabó Cs., Solberg T. N., and Bodnar R. J. (1994) Geochemical study of silicate melt inclusions in upper mantle xenoliths from the Nógrád-Gömör Volcanic Field (North Hungary/South Slovakia). *5th biennial PACROFI, Prog. Abstr.*, 103.

Yund R. A. and Kullerud G. (1966) Thermal stability of assemblages in the Cu-Fe-S system. *J. Petrol.* **7,** 454–488.